Journal of Sound and Vibration (2001) **246**(1), 137–155
doi:10.1006/jsvi.2001.3572, available online at http://www.idealibrary.com on IDEAL®

INFLUENCE OF LOW MACH NUMBER SHEAR FLOW ON ACOUSTIC PROPAGATION IN DUCTS

V. PAGNEUX

Laboratoire d'Acoustique del l'Université du Maine, UMR 6613 *CNRS, Avenue Oliver Messiaen* 72085 *Le Mans Cedex* 9, *France. E-mail: vincent.pagneux@univ-lemans.fr*

AND

B. FROELICH

Gas Engineering Montrouge, Schlumberger, 50 *Avenue Jean Jaurès*, 92 *Montrouge, France*

(*Received* 21 *August* 2000, *and in final form* 25 *January* 2001)

An experimental and theoretical investigation of the influence of a parallel shear flow on the sound propagation in a circular duct is described. The theoretical model is based on a perturbation expansion at low Mach number of the modal equation for parallel shear flows (Pridmore-Brown equation). In this model one assumes a rigid wall and no viscous or thermal effects. The experimental study was performed at low Mach number ($M < 0{\cdot}05$) with two propagating acoustic modes, and the Reynolds number range ($0 < \mathrm{Re} < 8500$) allowed various profiles for the mean flow. Measurement of the pressure gave the behaviour of the axial wavenumber of modes 0 and 1 that were propagating in our experiment. A good agreement between experimental and theoretical results was obtained.

1. INTRODUCTION

This paper contributes to the study of acoustic propagation in ducts having parallel mean shear flow at low Mach number. This subject is of considerable interest in industrial problems such as noise propagation in aircraft turbofan ducts or noise transmission in machinery involving fluid flow, and has been discussed several times in the literature. The earliest study appears to be that of Pridmore-Brown [1], who established a modal equation governing the transverse modes in parallel shear flow ducts. This equation is the compressible counterpart of the classical Rayleigh equation known in incompressible parallel flow instability theory [2]. It is therefore referred to either as the Pridmore-Brown equation or the compressible Rayleigh equation. It should be noted that the same equation is found in shallow water theory [3].

Following the paper by Pridmore-Brown, a series of papers dealt with this problem [4–10], often motivated by the question of attenuation in lined ducts. In this same period, Peube and Jallet [11] also devised a perturbation expansion technique to find the modes and corresponding wavenumber at low Mach number. More recently, Ko [12] and Nagel and Brand [13] proposed alternative approaches to the numerical solution of the Pridmore-Brown equation. Agarwal and Bull [14] have also made a complete analysis of many properties of axisymmetric and non-axisymmetric modes and wavenumbers, Gogate and Munjal [15] proposed approximate solutions, and Bihhadi and Gervais [16] recently

0022-460X/01/360137 + 19 $35.00/0

extended this treatment to take into account transverse temperature gradients. All of these studies were primarily concerned with numerical calculation of wavenumbers and transverse modes, and very few experimental results were presented to show the effect of shear flow on longitudinal wavenumbers of modes in ducts. Other authors have investigated theoretical aspects of a modal approach to shear flow duct problems. Swinbanks [17], Nilsson and Brander [18] and Mani [19] posed the problem of completeness of the transverse modes. In particular, Swinbanks analyzed the continuous set of modes that occur in the Pridmore-Brown problem due to the presence of internal singularities in the equation.

In this paper, both experimental and theoretical aspects of the multimodal acoustic propagation in shear flow ducts are presented. The geometry considered is a circular duct and the conditions are assumed to be axisymmetric throughout the paper. The theoretical model presented is based on an asymptotic expansion at low Mach number of the solution of the Pridmore-Brown equation. The expansion enables one to obtain simple expressions for axial wavenumbers, transverse modes and cut-off frequencies for any mean flow profile. Results from these asymptotic expressions are then compared with numerical computations and experimental results. The basis for the experimental results is the measurement of phase difference between source and receiver in a circular duct with mean flow. Measured phases are processed to give experimental values of wavenumbers for Mach number below 0·05, which can be compared with the theoretical results.

The paper is organized as follows: in section 2, the modal approach problem for propagation in mean shear flow is formulated. The theoretical treatment based on perturbation expansion in the low Mach number is presented in section 3. Section 4 describes the experimental set-up and protocol and presents initial experimental results. Section 5 contains the comparison between the experimental and theoretical parts, and concludes with a proposition for a simple method to reconstruct the mean flow profile from the acoustic measurement.

2. MODEL PROBLEM

Consider a circular duct of radius R with rigid walls, in which there is a parallel shear flow with axial velocity $U(r)$ (see Figure 1).

The governing equations for axisymmetric infinitesimal perturbations are the linearized Euler and mass conservation equations (upon neglecting visco-thermal effects)

$$\rho_0 \left(\frac{\partial u}{\partial t} + U \frac{\partial u}{\partial z} + v \frac{\mathrm{d}U}{\mathrm{d}r} \right) = - \frac{\partial p}{\partial z}, \tag{1}$$

$$\rho_0 \left(\frac{\partial v}{\partial t} + U \frac{\partial v}{\partial z} \right) = - \frac{\partial p}{\partial r}, \tag{2}$$

$$\frac{\partial \rho}{\partial t} + U \frac{\partial \rho}{\partial z} = - \rho_0 \left(\frac{\partial u}{\partial z} + \frac{1}{r} \frac{\partial rv}{\partial r} \right), \tag{3}$$

having boundary condition $\partial p/\partial r = 0$ for $r = R$, where u and v are the axial and radial components of acoustics velocity, p is the acoustic pressure, ρ the acoustic density and ρ_0 the mean density.

By assuming adiabatic conditions, the relation between ρ and p (equation of state) is

$$\frac{\mathrm{D}\rho}{\mathrm{D}t} = \frac{1}{c_0^2} \frac{\mathrm{D}p}{\mathrm{D}t}, \tag{4}$$

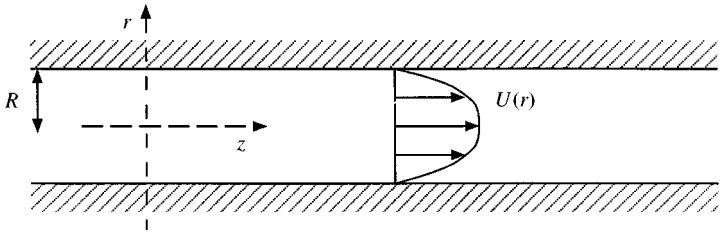

Figure 1. Geometry of the problem.

where c_0 is the sound speed at ambient temperature and $(\mathrm{D}/\mathrm{D}t) = \partial/\partial t + U\,\partial/\partial z$ is the convective differentiation operator.

Taking the divergence of equations (1, 2) and the convective differential of equation (3), one obtains

$$\frac{1}{c_0^2}\frac{\mathrm{D}^2 p}{\mathrm{D}t^2} - \Delta p = 2\rho_0 \frac{\mathrm{d}U}{\mathrm{d}r}\frac{\partial v}{\partial z}. \tag{5}$$

This is not a wave equation for the pressure p since the source term depends on the transverse velocity v and consequently on p, but a genuine wave equation can be obtained by differentiating equation (5) once again; then

$$\frac{\mathrm{D}}{\mathrm{D}t}\left(\frac{1}{c_0^2}\frac{\mathrm{D}^2}{\mathrm{D}t^2} - \Delta\right) p = -2\frac{\mathrm{d}U}{\mathrm{d}r}\frac{\partial^2 p}{\partial r \partial z}. \tag{6}$$

Incidentally, a particular effect of the presence of shear flow can be noticed in equation (6); the equation for the pressure is not second order as in the classical case, but is third order. This increase in the order of the wave equation reflects the enlargement of the set of solutions to include "hydrodynamic" solutions and the complex interaction between the flow and the acoustic wave [17].

In the modal approach, the acoustic quantities are written as

$$p(r, z) = P(r)\,\mathrm{e}^{\mathrm{j}(\omega t - \beta z)}, \qquad u(r, z) = A(r)\,\mathrm{e}^{\mathrm{j}(\omega t - \beta z)}, \qquad v(r, z) = B(r)\,\mathrm{e}^{\mathrm{j}(\omega t - \beta z)} \tag{7–9}$$

and one then obtains the Pridmore–Brown equation (PBE)

$$\Delta_\perp P + \frac{2M'}{k - M\beta}\beta P' + ((k - M\beta)^2 - \beta^2)\,P = 0, \tag{10}$$

where $\Delta_\perp = \partial^2/\partial r^2 + (1/r)\partial/\partial r$ is the transverse Laplacian, primes denote differentiation $\mathrm{d}/\mathrm{d}r$, $k = \omega/c_0$ and $M = U(r)/c_0$ is the local Mach number. The problem is then to solve equation (10) in terms of eigenvalues β and eigenfunctions P to obtain the wavenumbers and modes.

When made dimensionless, equation (10) can be written as

$$\Delta_\perp P + \frac{2M'}{1 - KM} KP' + \Omega^2\,((1 - KM)^2 - K^2)\,P = 0. \tag{11}$$

where the radial co-ordinate r is made dimensionless by R, $\Omega = kR$ and $K = \beta/k$. In the following, this dimensionless form of the equation will be used.

Except for the case of uniform flow, there are usually no analytical solutions to equation (10). Furthermore, once numerical solutions have been determined, it is impossible to

establish the completeness of the modes because equation (10) is not of the regular Sturm–Liouville type. A singularity is associated with the factor $1/(1 - KM)$ in front of the first derivative of P and it is responsible for the presence of a continuous set of eigenvalues $K \in [1/M_{max}, \infty)$, in addition to the classical discrete set [17, 19]. The following is restricted to the study of the classical discrete eigenvalues, and K_n and P_n correspond, respectively, to the eigenvalue and eigenvector of mode n.

3. THEORETICAL APPROACH: PERTURBATION EXPANSION

3.1. INTRODUCTION

Starting from the PBE with the hard wall boundary condition, the eigenvalue K and the eigenfunction P are expanded with respect to M as follows. First one notes that

$$M(r) = M_0 m(r), \tag{12}$$

such that $1/S \int_S m \, dS = \int_0^1 m(r) 2r \, dr = 1$ and $M_0 \ll 1$, and then K and P are expanded as

$$K_n = K_{0n} + M_0 K_{1n} + M_0^2 K_{2n} + \cdots, \tag{13}$$

$$P_n = P_{0n} + M_0 P_{1n} + M_0^2 P_{2n} + \cdots, \tag{14}$$

where the averaged Mach number is $M_0 = U_m/c_0$, with $U_m = Q/S$ where Q is the flow rate and S the cross-sectional area.

These expansions when introduced into the PBE yield a series of linear problems at each order (for frequencies far from cut-off, the case of the cut-off frequencies will be treated in a later section).

At order 0,

$$\Delta_\perp P_{0n} + \Omega^2 (1 - K_{0n}^2) P_{0n} = 0, \qquad P'_{0n}(1) = 0. \tag{15, 16}$$

At order 1 (M_0),

$$\Delta_\perp P_{1n} + \Omega^2 (1 - K_{0n}^2) P_{1n} = 2\Omega^2 K_{0n} (K_{1n} + m) P_{0n} - 2m' K_{0n} P'_{0n}, \tag{17}$$

$$P'_{1n}(1) = 0. \tag{18}$$

At order 2 (M_0^2),

$$\Delta_\perp P_{2n} + \Omega^2 (1 - K_{0n}^2) P_{2n} = 2\Omega^2 K_{0n} (K_{1n} + m) P_{1n} - 2m' K_{0n} P'_{1n}$$

$$- \Omega^2 [m^2 K_{0n}^2 - 2K_{0n} K_{2n} - K_{1n} (K_{1n} + 2m)] P_{0n} - 2m' (K_{1n} + mK_{0n}^2) P'_{0n}, \tag{19}$$

$$P'_{2n}(1) = 0. \tag{20}$$

At each order l ($l = 1, 2, 3, \ldots$,) the linear problem is of the form

$$L_n P_{ln} = f_l (P_{0n}, P'_{0n}, \ldots, P_{l-1n-1}, P'_{l-1n-1}).$$

The operator $L_n = \Delta_\perp + \Omega^2 (1 - K_{0n}^2)$ is self-adjoint, and thus the classical condition of solvability can be applied; this requires that each right-hand term f_l is orthogonal to the solution of the homogeneous problem $L_n P_{ln} = 0$. By noting that this latter is P_{0n}, this yields $\iint_S f_l P_{0n} \, dS = 0$. Thus, by using this condition it is possible to get the values K_{1n}, K_{2n}, etc. … .

In what follows, only the expansion at first order is treated. The expression for K_{1n} is found to be

$$K_{1n} = -\langle P_{0n}|mP_{0n}\rangle + \frac{1}{\Omega^2}\langle m'P'_{0n}|P_{0n}\rangle, \tag{21}$$

where the scalar product is defined by $\langle f\,|\,g\rangle = \int_0^1 f(r)g(r)\,2r\,\mathrm{d}r$ and where the normalization of P_{0n} is $\langle P_{0n}\,|\,P_{0n}\rangle = 1$. Equation (21) is the most important result of the theoretical part because it allows one to express the wavenumber in a simple form. An almost similar result was obtained in reference [11], but with an error due to the omission of the second term on the right-hand side of equation (21).

3.2. PROJECTION OF P_{1n}

To first order perturbation, the system of differential equations is reduced to equations (15)–(18). Problem (15) is equivalent to finding the transverse mode without mean flow, and one obtains

$$K_{0n}^2 = 1 - \gamma_n^2/\Omega^2 \text{ and } P_{0n} = C_n \mathrm{J}_0(\gamma_n r)$$

for the nth mode, where γ_n is the nth zero of $\mathrm{J}_1(x) = 0$, $(n \geqslant 0)$. The constant C_n is chosen so as to normalize P_{0n} such that $\langle P_{0n}\,|\,P_{0n}\rangle = 1$; hence $C_n = 1/\mathrm{J}_0(\gamma_n)$.

In order to obtain the solution P_{1n} corresponding to mode n, one projects P_{1n} on the functions $\psi_q = \mathrm{J}_0(\gamma_q r)/\mathrm{J}_0(\gamma_q) = P_{0q}$:

$$P_{1n}(r) = \sum_{q \geqslant 0} A_{nq}\psi_q(r).$$

Inserting this projection into equation (17) yields

$$A_{nq} = \frac{2\sqrt{1-\gamma_n^2/\Omega^2}}{(\gamma_n^2 - \gamma_q^2)}\left(\Omega^2\langle\psi_n\,|\,m\psi_q\rangle - \langle\psi'_n\,|\,m'\psi_q\rangle\right) \tag{22}$$

for $n \neq q$. It can be noted that the coefficient A_{nn} is a degree of freedom; it is chosen so that P is normalized according to $\langle P_n\,|\,P_n\rangle = 1 + O(M_0^2)$. At this point, a restriction on the perturbation expansion is evident because of the proportionality of A_{nq} to Ω^2. Indeed, for every high frequency, $\Omega \to \infty$ and A_{nq} terms diverge. That means that the development $P_n = P_{0n} + M_0 P_{1n} + \cdots$ is no longer valid since $M_0 P_{1n}$ cannot be neglected when compared to P_{0n}.

Equation (22) provides one with the coefficients $\langle P_{0n}\,|\,P_{1n}\rangle$, and thus could be used to obtain K_{2n} from the scalar product of equation (19) by P_{0n}; that would extend the approximation to the second order in the Mach number.

It may be noted, using vectorial notation, that the new transverse eigenfunctions (with shear flow) may be written as a function of the eigenfunction without flow,

$$\boldsymbol{\phi} = (I + M_0 A)\,\boldsymbol{\psi},$$

where $\boldsymbol{\phi} = (P_n)_{n \geqslant 0}$, $\psi_n = \mathrm{J}_0(\gamma_n r)/\mathrm{J}_0(\gamma_n)$ and the matrix A has components A_{nq}. For sufficiently small M_0, one might think that this relation may be inverted. In such a case, an approximated relation between the modes without and with shear flow would be obtained, and this property would suggest completeness of the transverse modes with shear flow. Nevertheless, it is mathematically dubious because of the continuous spectrum which is present when there is shear flow [17].

3.3. CUT-OFF FREQUENCIES

So far, the analysis has been performed for frequencies away from the cut-off frequencies of the modes without shear flow. That means that Ω has been given a fixed value different from γ_n, or, differently stated, that Ω was not of the form $\Omega = \gamma_n(1 + \varepsilon(M_0))$ with $\varepsilon \to 0$ when $M_0 \to 0$. If this condition is not satisfied one may assume that one is near the cut-off frequency of the mode n ($n \geqslant 1$) and write

$$\Omega^2 = \gamma_n^2 (1 - \eta M_0^2),$$

where η is a constant to be determined, and one looks at the value of K_{1n} for the mode n. The term in M_0, assumed square, is deduced from the expansion of the cut-off frequencies in the uniform flow case when $M_0 \ll 1$, which is $\Omega_{cn} = \gamma_n(1 - M_0^2/2)$.

Then equation at order zero (M_0^0) becomes

$$\Delta_\perp P_{0n} + \gamma_n^2 (1 - K_{0n}^2) P_{0n} = 0, \qquad P'_{0n}(1) = 0, \tag{23, 24}$$

which yields $K_{0n} = 0$ and $P_{0n} = \mathrm{J}_0(\gamma_n r)/\mathrm{J}_0(\gamma_n)$.

The equation for order one and two become

$$\Delta_\perp P_{1n} + \gamma_n^2 (1 - K_{0n}^2) P_{1n} = 0, \qquad P'_{1n}(1) = 0 \tag{25, 26}$$

and

$$\Delta_\perp P_{2n} + \gamma_n^2 (1 - K_{0n}^2) P_{2n} = \gamma_n^2 (\eta + K_{1n}(K_{1n} + 2m)) P_{0n} - 2m' K_{1n} P'_{0n}, \tag{27}$$

$$P'_{2n}(1) = 0. \tag{28}$$

Equation (27) contains a new term on the right-hand side that is due to the assumed expression for Ω^2. Then to obtain K_{1n}, the solvability condition must be applied to equation (27) (for second order) rather than equation (26) (for first order) as previously.

Eventually, one obtains

$$K_{1n} = K_{1n,cl} \pm \sqrt{K_{1n,cl}^2 - \eta}, \tag{29}$$

where $K_{1n,cl} = -\langle P_{0n} | m P_{0n} \rangle + 1/\gamma_n^2 \langle m' P'_{0n} | P_{0n} \rangle$ is the value corresponding to the classical situation (equation (21)) with Ω equal to γ_n.

Then, the cut-off frequency corresponds to the case where there is a unique solution for this equation (cf. reference [16]): i.e., it corresponds to $\eta = K_{1n,cl}^2$. By substituting this expression for η in the expression of Ω, the cut-off frequencies are found to be

$$\Omega_{cn} = \gamma_n \left(1 - \frac{K_{1n,cl}^2}{2} M_0^2\right) + o(M_0^2). \tag{30}$$

Obviously, this value is different from the one obtained without flow ($\Omega_{cn} = \gamma_n$) and that obtained for uniform flow, because of the effect of shear in the flow, and it depends on $K_{1n,cl}$ and γ_n.

3.4. RESULTS

The first consequence of the analytical analysis developed in the previous section concerns the first mode, referred to as mode 0. Indeed, from equation (21), it can be seen that the expression of K_{10} does not depend on the form of the means flow profile: always $K_{10} = -1$. Thus, to a first order with respect to M_0, the mode 0 wavenumber is

$$K_0 = K_{00} - M_0$$

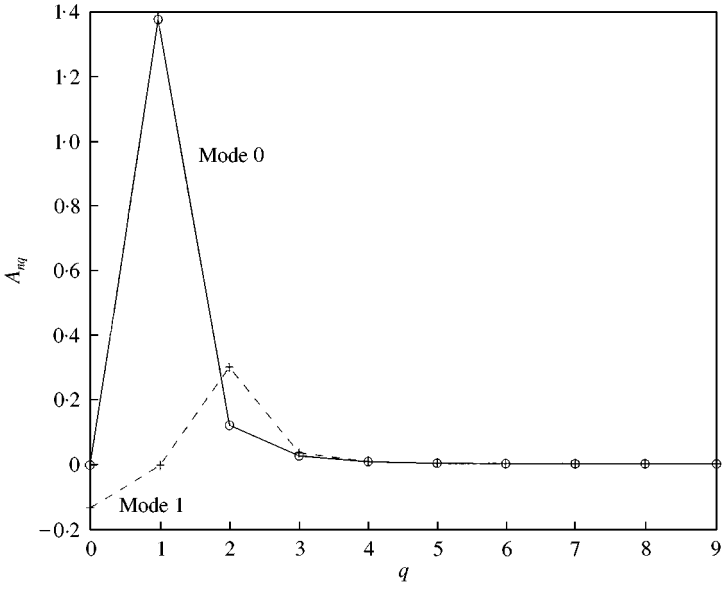

Figure 2. Projection coefficients for mode 0 (A_{0q}) and mode 1 (A_{1q}) as a function of q, $\Omega = 4{\cdot}3$.

with $K_{00} = \pm 1$. So mode 0 is simply convected by the average of the shear mean flow as far as first order in the Mach number is concerned.

For higher order modes (mode 1, 2, etc, …), the situation is more complicated because P_{0n} is not a constant function of r, and a particular mean flow profile must be chosen. For the case of a parabolic mean flow profile this corresponds to $m(r) = 2(1 - r^2)$ with $r \leqslant 1$ (the factor of 2 ensures that $1/S \int m \, \mathrm{d}S = 1$). K_{1n} is then calculated analytically from equation (21) as

$$K_{1n} = -\tfrac{4}{3}$$

by using two integrals of the forms $\int_0^1 t^3 \, \mathrm{J}_0^2(\gamma_n t) \, \mathrm{d}t = \frac{1}{6} \, \mathrm{J}_0^2(\gamma_n)$ and $\int_0^1 t^2 \, \mathrm{J}_0(\gamma_n) \, \mathrm{J}_1(\gamma_n t) \, \mathrm{d}t = 0$ [20], and this shows that, for a parabolic mean flow profile, the wavenumbers of the higher order modes ($n \geqslant 1$) to the first order in Mach number are

$$K_n = K_{0n} - \tfrac{4}{3} M_0, \tag{31}$$

where $K_{0n} = \pm \sqrt{1 - \gamma_n^2/\Omega^2}$. The perturbation is the same for all the higher order modes and characterized by the factor 4/3. One can note that for the parabolic profile, K_{1n} does not depend on the frequency Ω because $\langle m' P'_{0n} \, | \, P_{0n} \rangle = 0$. It can be noted that this factor 4/3 is also given by the empirical formula $K_n = K_{0n} - M_{eff}$ proposed in references [14, 21], with $M_{eff} = \int_0^1 M(r) \, \mathrm{d}r$, but it has been verified that this is true only for a parabolic profile (as far as polynomial profiles are concerned).

The coefficients A_{nq} for $n = 0$ (mode 0) and $n = 1$ (mode 1) are shown in Figure 2. They are very rapidly decreasing functions of q. That means that the projection of modes with flow on the modes without flow can be very efficient even with very few terms. Moreover, one can see that the magnitude of P_{1n} is much larger for mode 0 than for mode 1. Figures 3 and 4 show the behaviour of the profile for the pressure of modes 0 and 1, in the case of downstream propagation. As already observed by reference [1] for instance, the influence of the shear flow on the shape of the pressure profile is much more important for mode 0 than

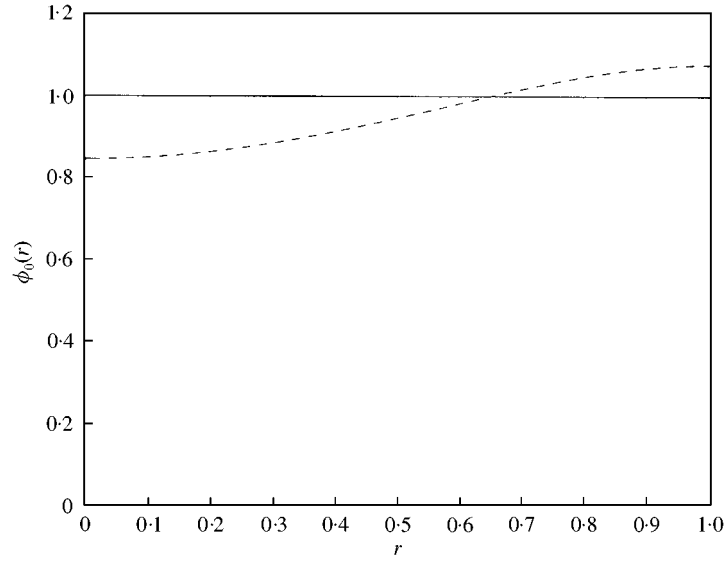

Figure 3. Acoustic profiles for mode 0: ———, without flow ψ_0; – – –, with parabolic profile flow ϕ_0 ($M_0 = 0{\cdot}05$ and $\Omega = 4{\cdot}3$).

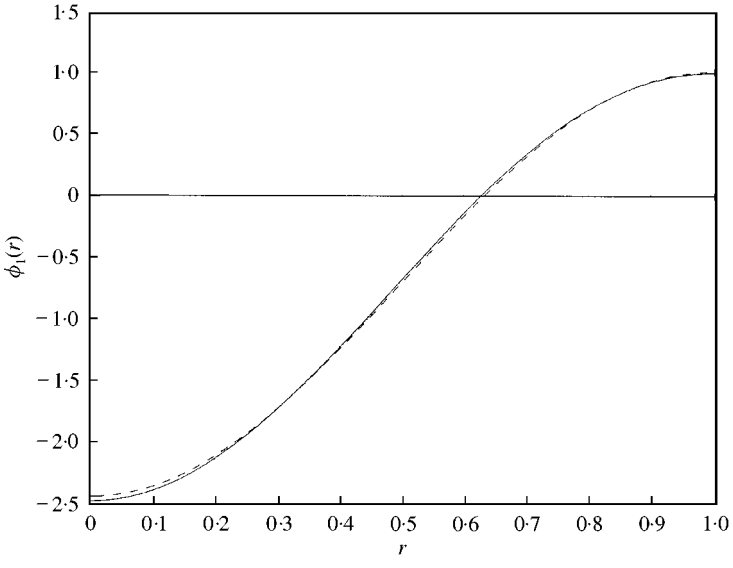

Figure 4. Acoustic profiles for mode 1: ———, without flow ψ_1; – – –, with parabolic profile flow ϕ_1 ($M_0 = 0{\cdot}05$ and $\Omega = 4{\cdot}3$).

for the higher order modes (in this case, mode 1). The cut-off frequencies with parabolic flow are obtained from equation (30)

$$\Omega_{cn} = \gamma_n \left(1 - \tfrac{8}{9} M_0^2\right). \tag{32}$$

The parabolic mean flow profile is quite representative for real situations with low Reynolds number $R_e = U_0 R/\nu$ (where U_0 is the averaged velocity over the cross-section of

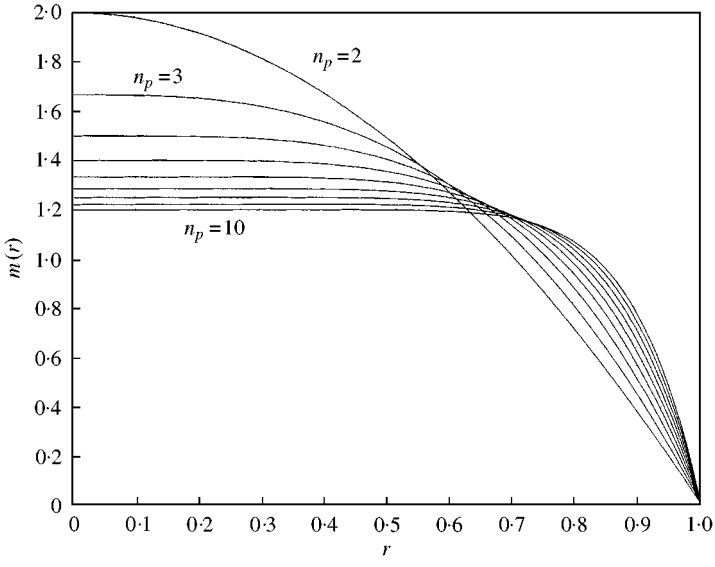

Figure 5. Mean flow profile for $n_p = 2$–10.

the duct and v the kinematic viscosity) of the mean flow, but as R_e increases the flow becomes turbulent and as a result the profile becomes flatter and flatter. In order to model for change in the profile in a simple manner, a family of profiles of the form

$$m(r) = \frac{n_p + 2}{n_p}(1 - r^{n_p})$$

is proposed. They have a constant average over the cross-section and become flatter and flatter as n_p is increased. This family of profiles is shown in Figure 5 for n_p between 2 and 10.

The perturbative parts of mode 0 and mode 1 profiles (P_{10} and P_{11}) are shown in Figures 6 and 7 for a given frequency, when the mean flow profiles are those proposed in Figure 5. P_{10} and P_{11} represent the distortion of the total acoustic profiles P_0 and P_1, and they decrease when n_p increases, i.e., when the mean flow profile becomes flatter and flatter for a given flow rate. Thus, the more the mean flow has shear, the more the mode profiles are distorted.

3.5. NUMERICAL CALCULATION

In order to verify the first order approximation (in Mach number) of the preceding analysis, a direct numerical integration of the PBE was carried out in the case of a parabolic mean flow profile. A fourth order Runge–Kutta method was used to integrate the PBE and to find the eigenvalue K_n, and the results are shown in Figures 8 and 9. These show both downstream and upstream wavenumbers K_n corresponding to propagating modes at the frequency under consideration, for Mach numbers up to 0·5. It can be seen that the first order approximation is valid for each mode for Mach numbers less than 0·05.

4. EXPERIMENTAL SET-UP AND RESULTS

The experimental set-up used allowed study of the axisymmetric acoustic propagation in a circular duct which was very long compared to the wavelength. The medium used was air

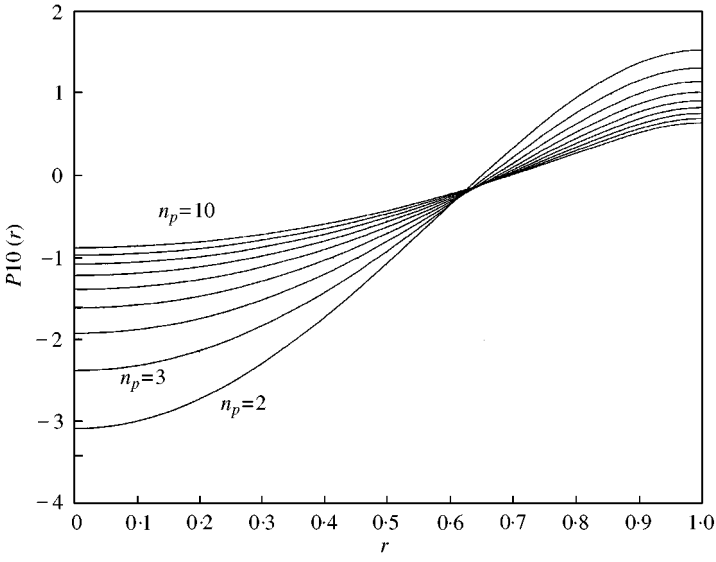

Figure 6. Perturbative part ($P_{10}(r)$) of the pressure for mode 0 for a range of mean flow profiles (n_p varies), $\Omega = 4{\cdot}3$.

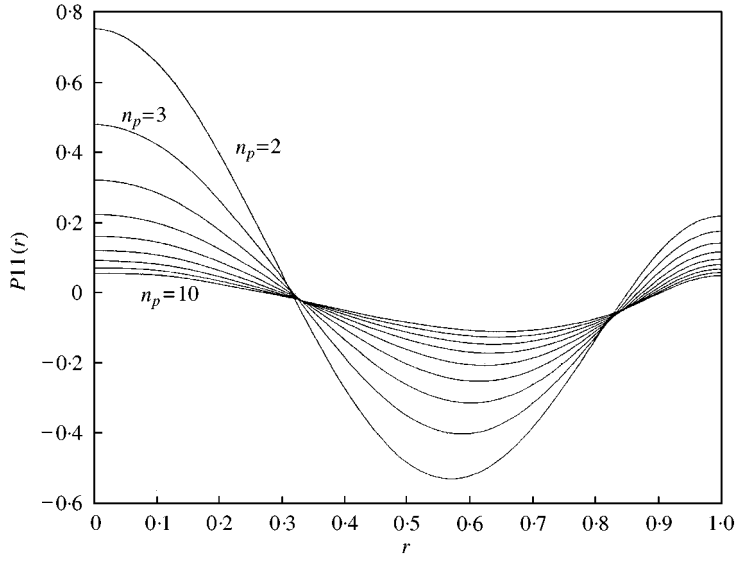

Figure 7. Perturbative part ($P_{11}(r)$) of the pressure for mode 1 with different mean flow profile (n_p varies), $\Omega = 4{\cdot}3$.

in which a mean flow was induced for low Mach numbers ($0 < M < 0{\cdot}05$, with $M = U_0/c_0$ where U_0 is the mean velocity over the cross-section of the duct and c_0 the sound speed). The aim was to observe the influence of the mean flow over the propagation in the duct without the effects of duct terminations. The study, therefore, was carried out in the temporal domain, using a short pulse, instead of the frequency domain, with a continuous source. Indeed, though it was desired to obtain measurements to compare with harmonic theory, the short pulse enabled one to avoid the reflected signals from the duct termination

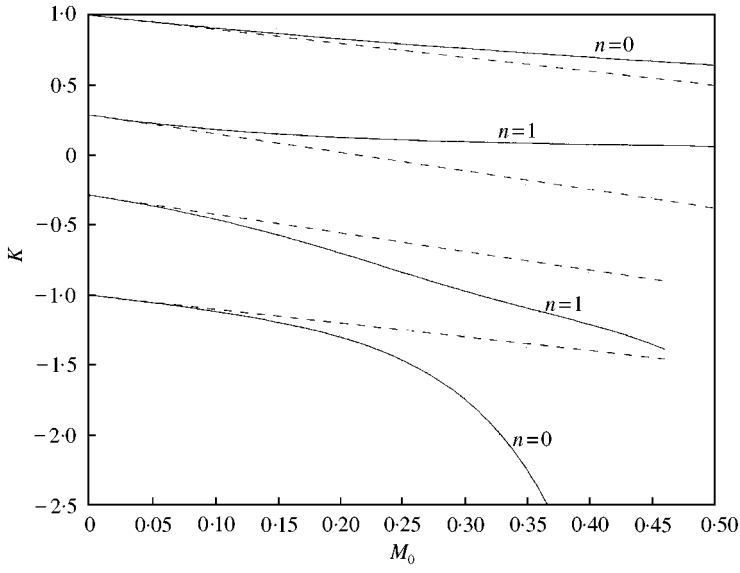

Figure 8. Downstream and upstream wavenumber K for mode 0 and mode 1 as a function of Mach number M_0. Parabolic mean flow profile and $\Omega = 4$: ———, numerical computation: – – –, first order approximation.

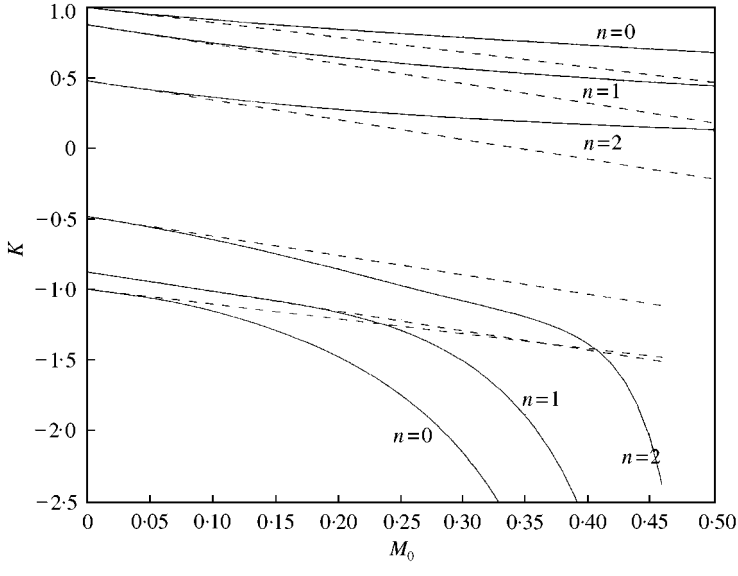

Figure 9. Downstream and upstream wavenumber K for mode 0, 1 and 2 as a function of Mach number M_0. Parabolic mean flow profile and $\Omega = 8$: ———, numerical computation: – – –, first order approximation.

since they can be separated from the direct signal. The reason for wishing to avoid taking account of the duct termination with a harmonic source is the difficulty of modelling the radiation impedance of an open-ended duct for instance.

For the range of Mach numbers considered, the Reynolds number ($\mathrm{Re} = U_0 R/v$ with R the radius of the duct and v the kinematic viscosity of air) ranges from very low values (Poiseuille flow) to about 8500 (turbulent flow). Hence, the flow profile in the duct takes

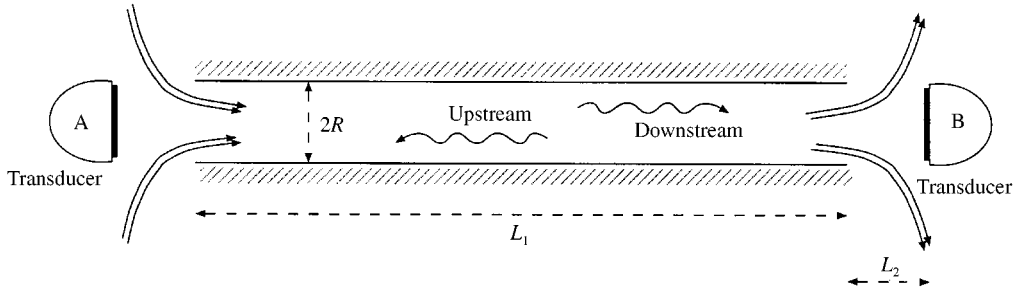

Figure 10. Scheme of the experiment: signals are emitted from A for downstream propagation and from B for upstream propagation.

a variety of shapes; for Re close to zero the profile is parabolic and for higher and higher values of Re up to 8500 the profile becomes flatter and flatter.

4.1. EXPERIMENTAL SET-UP AND FACILITIES

The principle of the experiment is presented in Figure 10: two transducers A and B capable of both emitting and receiving, are located at the two extremities of the circular duct of length (L_1) 110 cm and radius (R) 0·6 cm. The direction of flow is from A to B. The signal is emitted from A for downstream propagation and then received at B, then *vice versa* for upstream propagation.

The physical set-up is presented in Figure 11. The flow is induced by a descending piston which pushes air through the duct. The maximum pressure imposed by the piston in 30 mb relative to the atmospheric pressure. If one assumes the air to be incompressible (since $M < 0{\cdot}05$), the flow rate can be satisfactorily obtained by measuring the rate of movement of the piston.

The piston cylinder is connected to the cavity where transducer A is located. Next, the air goes through the duct at the outlet of which transducer B is placed. Then the air exits through a system of calibrated vanes which are used to control the flow rate. The two transducers are connected to a commutator which can interchange their roles of emitter and receiver. This commutator is connected both to a high frequency generator and an amplifier and digital analyzer. This latter outputs to a personal computer for data collection.

4.2. PARAMETERS

The distance L_2 between each of the transducers and the duct needs to be chosen to minimize the pressure loss caused by the transducer constricting the flow. However, if L_2 is too large mode 1 is not excited sufficiently in the duct since the spatial shape of the wave is too flat and hence too close to the shape of mode 0 at the entrance of the duct. Thus, a compromise was found which gave acceptable pressure loss of the mean flow and excitation of mode 1 in the duct. With this compromise value for L_2 the range of flow rates proved to be from 0 to 7000 l/h corresponding to a maximal mean flow velocity of about 17 m/s.

The central frequency of the excited pulse has been chosen so as to give two propagating modes in the duct ($kR > 3{\cdot}83$). To avoid propagating modes that are not axisymmetric the sources have been placed as axisymmetrically as possible. Another constraint on the

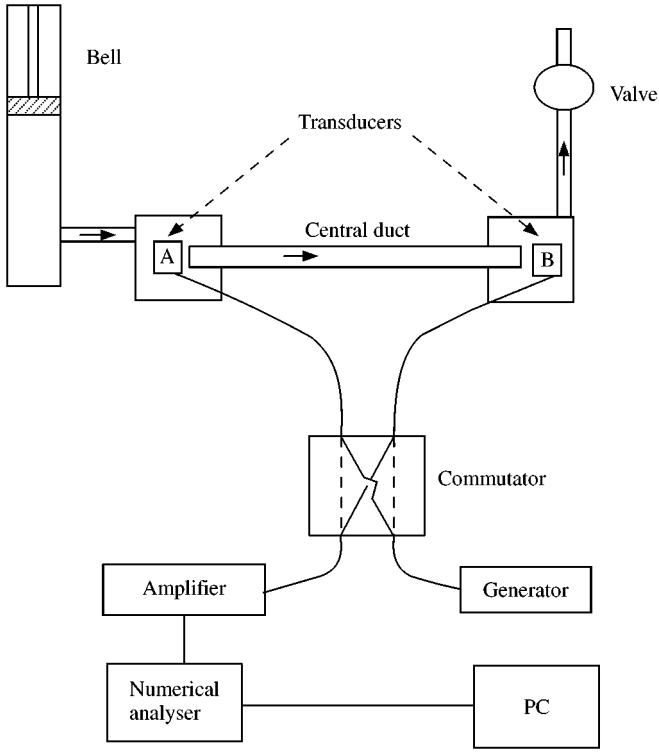

Figure 11. Experimental set-up; areas through which the flow goes are darkened.

frequency arises from the need to be able to separate the two propagating modes in the received signal; it has to be such that the group velocity of the two modes are sufficiently different. If this is well done, the wave packet of mode 0 is separated from the packet of mode 1. In the experiment, $kR \sim 4{\cdot}3$ was chosen.

Figure 12 shows the received signal at B in the absence of mean flow. It can be seen that the two wave packets are well separated and allow one to select unambiguously the parts corresponding to the two modes (i.e., mode 0 and mode 1). The times of arrival are $t_1 = L/c_0$ for the first packet and $t_2 = L/v_g \simeq 2t_1$ for the second packet. The sensitivities of the transducers were adjusted so that the signal received at A (B emitter) was the same as that represented in Figure 12 for the receiver at B (A emitter). So, in the presence of mean flow, the difference between the upstream and the downstream propagation is due only to the effect of the mean flow. Results obtained for a Mach number of 0·02 are presented in Figure 13 where it can be noted that the signal propagated downstream has a shorter time of arrival than the upstream one. This is simply due to the convection effect of the mean flow.

For mode 0, the measurement was performed in two steps; first, a time window was chosen to select only the first wave packet, and second a FFT was taken in this window and this gives the phase due to the propagation between the emitter and the receiver at the dominant frequency of the emitted signal (40 kHz). The same procedure was repeated after swapping the roles of emitter and receiver of A and B to obtain the result of downstream propagation. Taking the difference between the downstream and upstream phase $\Delta\phi = \phi_d - \phi_u$ shows the effect of the mean flow. The procedure is the same for mode 1 except that a different time window is taken to pick out only the second wave packet. At

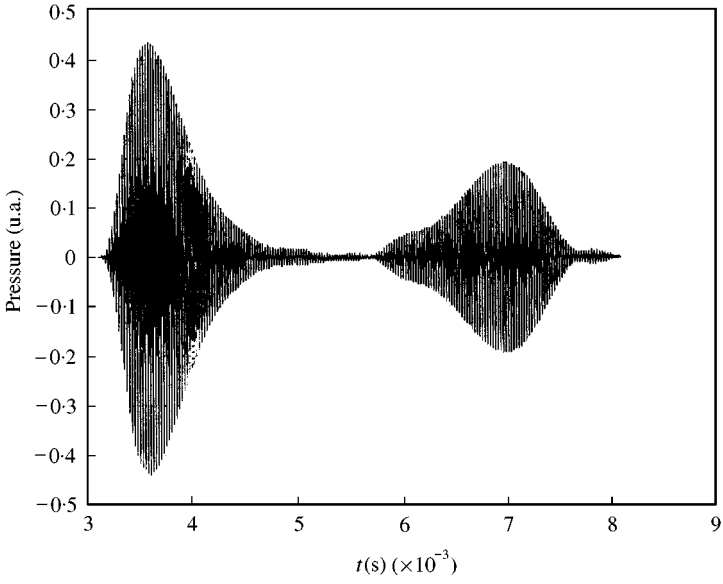

Figure 12. Temporal signal at the receiver without flow.

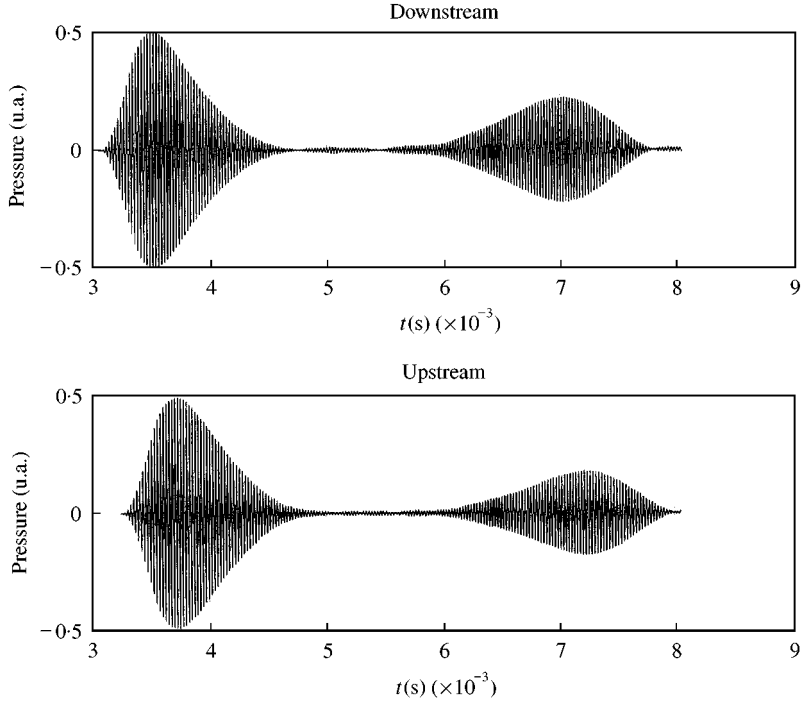

Figure 13. Comparison between signals at the receiver for downstream and upstream propagation, $M_0 = 0{\cdot}02$.

each combination of flow rate and selected mode an average of over 100 measurements were made and the standard deviation did not exceed 2%.

The phase differences $\Delta\phi$ are presented in Figure 14 which shows that for both modes $\Delta\phi$ increased with the Mach number. The slope for mode 0 is quite constant but, for mode 1, some change in the slope can be observed.

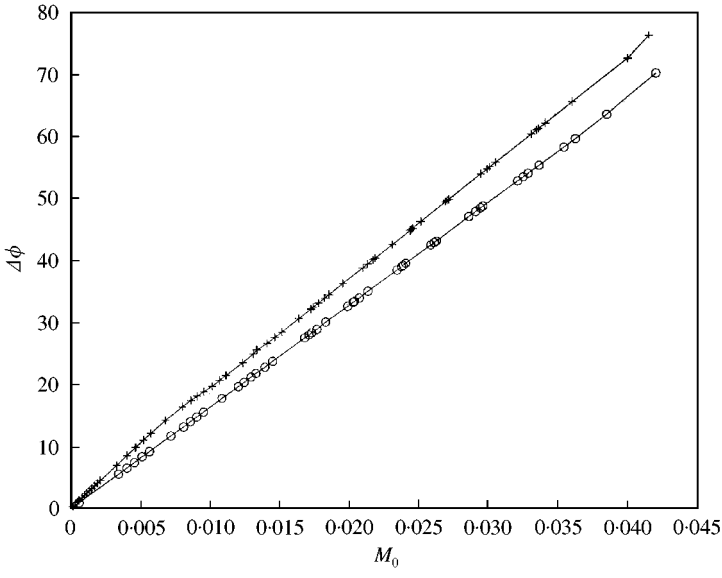

Figure 14. Upstream–downstream phase difference, $\Delta\phi = \phi_d - \phi_u$ for mode 0 (○) and for mode 1 (+), as functions of Mach number.

5. COMPARISON BETWEEN THEORY AND EXPERIMENT

The perturbation theory of section 3 enables one to express the approximations for the downstream and upstream phases for mode n as

$$\phi_d = -kL_1(K_{0n} + K_{1n}M_0), \qquad \phi_u = -kL_1(K_{0n} - K_{1n}M_0),$$

which yield ($\Delta\phi_n = \phi_d - \phi_u$ for mode n)

$$\Delta\phi/M_0 = -K_{1n}C_0, \tag{33}$$

where $C_0 = 2kL_1$ and K_{1n} is as expressed by equation (21). The factor C_0 depends only on frequency, temperature and length of the duct. Since it does not vary with the mean flow, it is considered here only as a normalization constant. $\Delta\phi_n/M_0$ is normalized by its mean value for mode 0. That is to say that C_0 is experimentally determined by $\langle\Delta\phi_0/M_0\rangle$, and that one is looking at the quantity $\Gamma_n = \Delta\phi_n/M_0/\langle\Delta\phi/M_0\rangle = \Delta\phi_n/(C_0M_0)$.

Figure 15 shows the behaviour of the experimental values for Γ_n for modes 0 and 1 when the Mach number varied. It is seen that Γ_0 is fairly constant and approximately close to unity on the range of Mach numbers considered as predicted by the theory. On the other hand, for mode 1, Γ_1 is very close to 4/3, the theoretical value of $-K_{1n}$ for a parabolic profile, for M_0 close to zero. It is a consistent result because at such a low value of Mach number the mean flow profile is almost certainly parabolic. As M_0 is increased Γ_1 decreases from 1·33 to 1·1. It must be noted that the mean flow profile cannot be considered to be strictly constant in the experiment because of the inlet length L_e necessary for the mean flow profile to be established in the duct. By applying classical evaluation of this entry length [22], it can be seen that L_e should be maximum in the laminar-turbulent transition and then decrease sharply for fully developed turbulent flow. Nevertheless, the mean flow profile can be considered to be slowly changing on the scale of the acoustic wavelength, and in this case K_{1n} is expressed as a functional of $\bar{m}$ in equation (21), where $\bar{m}(r)$ is the averaged value of m along the duct. To model the fact that the mean flow profile changes from a parabolic

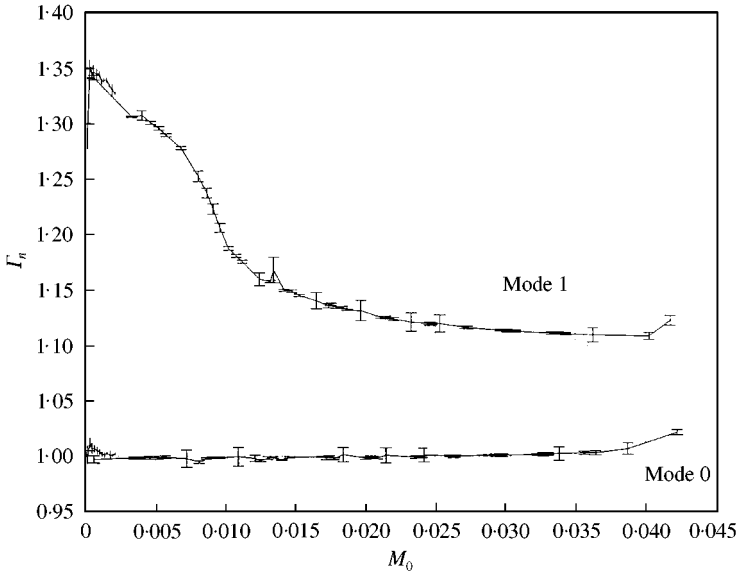

Figure 15. Experimental values of Γ_n for mode 0 ($n = 0$) and mode 1 ($n = 1$) as a function of Mach number.

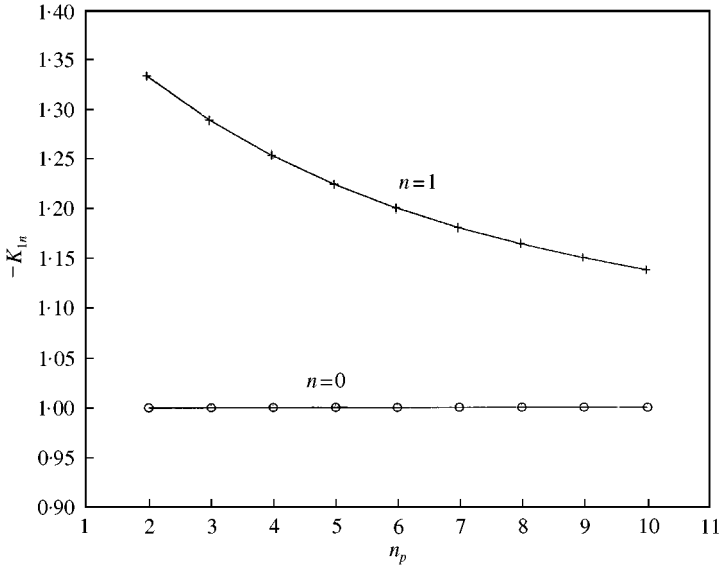

Figure 16. Theoretical values $-K_{1n}$ for mode 0 (○) and for mode 1 (+) as a function of n_p representing the shape of the mean flow profile.

shape for M_0 close to zero to turbulent shape (i.e., flat), the factor $-K_{1n}$ is shown in Figure 16 as a function of the integer number n_p characterizing the family of profiles $m(r) = (n_p + 2)/n_p\,(1 - r^{n_p})$ (cf. Figure 5). The qualitative behaviour of Γ_1 is recovered with this family of profiles, a fact that tends to confirm the validity of the theoretical model.

At this point, it seems possible to pose a kind of inverse problem for finding the mean flow profile from a knowledge of Γ_1. One assumes a profile shape of the form, where n is a chosen

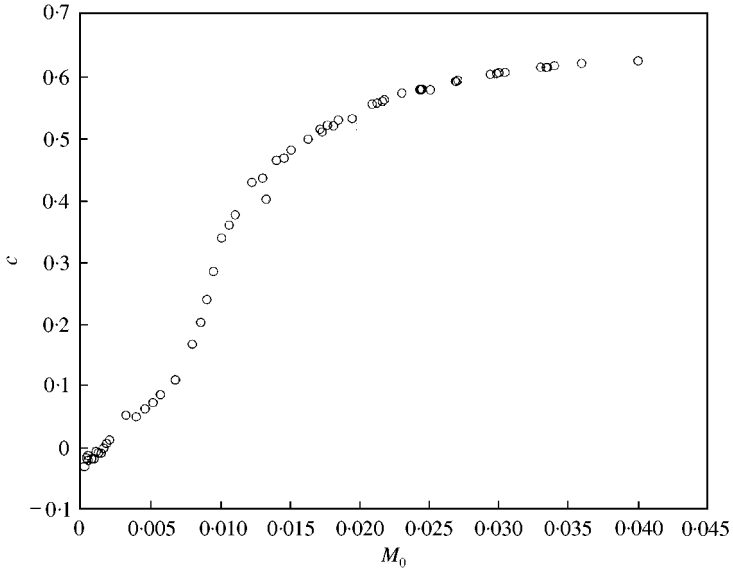

Figure 17. Coefficient c as a function of Mach number.

value,

$$m(r) = a(1 - (1 - c)r^2 - cr^n), \tag{34}$$

where $a = 1/(1 - (1 - c)/2 - 2c/(n + 2))$ in order that $\langle 1 \,|\, m \rangle = 1$. Then from the expression for K_{1n} (equation (21)) the only remaining unknown coefficient, c, can be shown to be

$$c = \frac{4 + 3K_{1n}}{-3(n-2)/(n+2)K_{1n} - 2(1 - 6I) - 12J/\Omega^2}, \tag{35}$$

where $I = \langle r^{n+1} P_{0n} \,|\, P_{0n} \rangle$ and $J = \langle nr^n P_{0n} \,|\, P'_{0n} \rangle$ are given integrals which have been numerically computed. If one assumes that K_{1n} is determined by the experimental value $\Gamma_n = -K_{1n}$, one can obtain the value for c from Γ_n and hence the profile of the mean flow (averaged all along the duct). It can be noted that if $K_{1n} = -4/3$, then $c = 0$ and the profile is parabolic. By trying several values of n in equation (34), it was found that $n = 40$ is a value suitable for approximating typical turbulent mean flow profile as the one proposed in reference [14]. With this value of n, Figure 17 shows the behaviour of the coefficient c as M_0 varies. As could be anticipated, for $M_0 \to 0$, c is very close to zero which means that the mean flow profile is nearly parabolic. For larger values of M_0, c increases to 0·7 confirming that the profile is becoming flatter because the parabolic part in the assumed profile is less and less important. Figure 18 presents the change of the mean flow profile as M_0 varies, and it illustrates the results that the inverse method is capable of giving.

6. CONCLUSION

The influence of shear flow on the acoustic propagation in a duct has been investigated, both theoretically and experimentally. A perturbation expansion is applied to obtain analytical forms for the wavenumbers of transverse modes at low Mach number, and this approximation is valid for $M_0 < 0{\cdot}05$. The results show that mode 0 is not sensitive to the

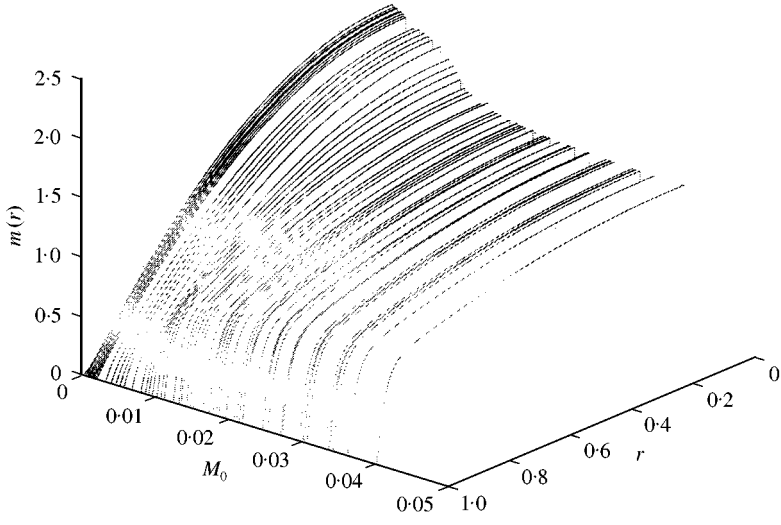

Figure 18. Set of mean flow profiles for different Mach number M_0 obtained by the inverse problem method.

specific shape of mean flow profile. The higher order modes, however, depend on the shape of the mean flow profile. These theoretical results compare favourably with experimental results, and an inverse treatment of experimental data is proposed for obtaining a measurement of the mean flow profile.

REFERENCES

1. D. C. PRIDMORE-BROWN 1958 *Journal of Fluid Mechanics* **4**, 393–406. Sound propagation in a fluid flowing through an attenuating duct.
2. BETCHOV and CRIMINALE 1965 *Stability of Parallel Flows*. New York: Academic Press.
3. S. TAKEHIRO and Y. HAYASHI 1992 *Journal of Fluid Mechanics* **236**, 259–279. Overreflection and shear instability in a shallow water model.
4. D. H. TACK and R. F. LAMBERT 1965 *Journal of the Acoustical Society of America* **38**, 655–666. Influence of shear flow on sound attenuation in a lined duct.
5. P. N. SHANKAR 1971 *Journal of Fluid Mechanics* **47**, 81–91. On acoustic refraction by duct shear layer.
6. P. N. SHANKAR 1972 *Journal of Sound and Vibration* **22**, 221–232. Sound propagation in duct shear layers.
7. P. N. SHANKAR 1972 *Journal of Sound and Vibration* **22**, 233–246. Acoustic refraction and attenuation in cylindrical and annular ducts.
8. S. D. SAVKAR 1971 *Journal of sound and Vibration* **19**, 355–372. Propagation of sound in ducts with shear flow.
9. S. H. KO 1973 *Journal of the Acoustical Society of America* **54**, 1592–1606. Theoretical prediction of sound attenuation in acoustically lined annular ducts in the presence of uniform flow and shear flow.
10. A. H. NAYFEH, J. E. KAISER, and B. S. SHAKER 1974 *Journal of Sound and Vibration* **34**, 413–423. Effect of mean-velocity profile shapes on sound transmission through two-dimensional ducts.
11. J. L. PEUBE and M. F. JALLET 1973 *Acoustica* **29**, 82–92. Propagation d'ondes acoustiques dans un écoulement en conduite cylindrique.
12. S. H. KO 1981 *Journal of the Acoustical Society of America* **70**, 205–212. New approach to the solution of eigenvalue problems in circular flow ducts (a Taylor series method).
13. R. T. NAGEL and R. S. BRAND 1982 *Journal of Sound and Vibration* **85**, 19–29. Boundary layer effects on sound in a circular duct.

14. N. K. AGARWAL and M. K. BULL 1989 *Journal of Sound and Vibration* **132**, 275–298. Acoustic wave propagation in a pipe with fully developed turbulent flow.
15. G. R. GOGATE and M. L. MUNJAL 1993 *Journal of Sound and Vibration* **160**, 465–484. Analytical solution of sound propagation in lined or unlined circular ducts with laminar mean flow.
16. A. BIHHADI and Y. GERVAIS 1994 *Acta Acoustica* **2**, 343–357. Propagation in duct with mean flow and temperature gradients.
17. M. A. SWINBANKS 1975 *Journal of Sound and Vibration* **40**, 51–76. The sound field generated by a source distribution in a long duct carrying sheared flow.
18. B. E. NILSSON and O. BRANDER 1980 *Journal of the Institute of Mathematics and its Applications* **26**, 269–298. The propagation of sound in cylindrical ducts with mean flow and bulk-reacting lining.
19. R. MANI 1980 *Proceedings of the Royal Society London A* **371**, 393–412. Sound propagation in parallel sheared flows ducts: the mode estimation problem.
20. V. PAGNEUX, N. AMIR and J. KERGOMARD 1996 *Journal of the Acoustical Society of America* **100**, 2504–2517. A study of wave propagation in varying cross-section waveguides by modal decomposition—Part I: theory and validation.
21. M. N. MIKHAIL and A. N. ABDELHAMID 1973 *American Institute of Aeronautics and Astronautics Paper*, 73–1013, 1–14. Transmission and far-field radiation of sound waves in and from lined ducts containing shear flow.
22. F. M. WHITE 1986 *Fluid Mechanics*. New York: McGraw-Hill International Editions, second edition.